Matthews, M. B., Kearns, S. L., & Buse, B. (2018). The Accuracy of Al and Cu Film Thickness Determinations and the Implications for Electron Probe Microanalysis. *Microscopy and Microanalysis*, *24*(2), 83-92. https://doi.org/10.1017/S1431927618000193

The Accuracy of Al and Cu Film Thickness Determinations and the Implications for Electron Probe Micro-Analysis

Matthews, M.B.[1,2], Kearns, S.L.[2] and Buse, B.[2]

1. AWE, Reading, UK
2. University of Bristol, Bristol, UK

Abstract

The accuracy to which Cu and Al coatings can be determined, and the effect this has on the quantification of the substrate, is investigated. Cu and Al coatings of nominally 5, 10, 15 and 20nm were sputter coated onto polished Bi using two configurations of coater: One with the Film Thickness Monitor (FTM) sensor co-located with the samples, and one where the sensor is located to one side. The FTM thicknesses are compared against those calculated from measured Cu Lα and Al Kα k-ratios using PENEPMA, GMRFilm and DTSA-II. Selected samples were also cross-sectioned using Focussed Ion Beam (FIB).

Both systems produced repeatable coatings, the thickest coating being ~4 times the thinnest coating. The side located FTM sensor indicated thicknesses less than half those of the software modelled results, propagating on to 70% errors in substrate quantification at 5kV. The co-located FTM sensor produced errors in film thickness and substrate quantification of 10 – 20%. Over the range of film thicknesses and accelerating voltages modelled both the substrate and coating k-ratios can be approximated by linear trends as functions of film thickness. The Al films were found to have a reduced density of ~2gcm^{-2}.

Introduction

EPMA at low accelerating voltages and/or low over-voltages in the reach for ever higher resolution means that any surface coatings on samples can no longer be treated as an negligible part of the analysis volume. A good body of work exists on the analysis of the surface films themselves stretching back to the early years of EPMA (for example Anderson 1966; Hutchins 1966; Yakowitz & Newbury 1976; Waldo 1988; Pouchou & Pichoir 1990; Bastin et al. 1998; Statham 2010).

However, a relatively small subset of these papers focus on the analysis of the substrate. A risk for the analyst is that, where the film isn't the component of interest and the potential errors are not appreciated, the film will either not be accounted for at all or, for applied conductive coatings, the thickness values reported by the coater will be accepted without question. In this study we investigate the potential sources and magnitudes of errors that can be expected in substrate quantification as we move towards achieving higher resolution analysis at lower accelerating voltages. For example, Figure 1 shows plots of Bi Mα emitted intensities, calculated using DTSA-II software (Ritchie et al. 2008), for a pure Bi substrate coated with 5, 10, 15 and 20nm of C, over a range of accelerating voltages. At voltages of 7kv or greater the emitted k-ratio is largely unaffected by the C coat. However, at 5kV a

20nm coating reduces the k-ratio by about 10%. Reducing the accelerating voltage further, to 3kV, this same coating reduces the measured k-ratio by 80%. Even relatively high energy X-rays can be significantly reduced at moderate accelerating voltages: The Kα intensity from an Fe substrate is supressed by ~2% by only 20nm of C coating at 14 kV, increasing to 7% at 13 kV (values calculated using GMRFilm). Thus even a very low atomic number coating can have a significant impact on quantification. Kerrick et al. (1973) attributed 4% loss in emitted F Kα intensity from mineral samples analysed at 10kV to 20nm differences in C coating thicknesses between sample and reference materials, as a result of absorption by the coat. Energy loss of the primary electrons within the coat also reduces the energy available to fluoresce X-rays in the sample (Leder & Suddeth 1960). This latter effect is particularly relevant for low over-voltage analyses.

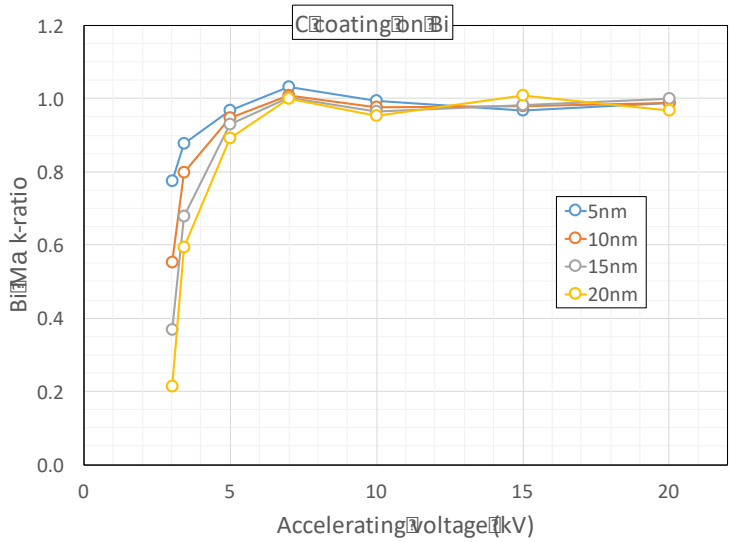

Figure 1 Bi Mα k-ratio from a pure Bi substrate, calculated using DTSA-II, as a function of accelerating voltage for a range of C coating thicknesses. At low accelerating voltages, even moderate thickness C coats can cause significant reductions in the measured substrate intensity.

Several studies have been carried out which at least partly involved investigating the accuracy of film thickness determinations using a range of techniques, such as Quartz Crystal Microbalance (QCM, also called a Film Thickness Monitor, FTM), Rutherford Backscattering (RBS), Optical Interferometry (OI), and Monte Carlo (MC). Table 1 shows a summary of the films measured, their ranges of thicknesses and the methods of measurements used for a non-exhaustive selection of such studies.

Unfortunately, determining the relatively simple parameter of the thickness of a pure element coating can be prone to significant errors: Bastin and Heijligers reported in their study that *"Establishing the real thicknesses of the films turned out to be a major problem"* (Bastin & Heijligers 2000a).

These earlier studies covered films of 100's of nm thick, with perhaps one or two measurements on films in the low 10's of nm, but it is this largely unrepresented lower end of the range that is of particular relevance for conductive coatings for electron microanalysis: Using the colour change from red to blue of a carbon coat deposited on a polished brass block yields a coating thickness of 20 – 25 nm (Kerrick et al. 1973); Goldstein et al state that C coats of only 5nm should provide sufficient electrical conductivity (Goldstein et al. 2003) but coatings in the range 10 – 20 nm are probably most common.

Study	Methods*							Coatings	Thicknesses (nm)
	QCM	OI	RBS	MC	Grav.	Opt.	XRR		
(Blois & Rieser 1954)	X	X						Cu, Ag	20 - 300
(Hartman 1965)	X	X						Al	25 - 200
(Lovell & Rollinson 1968)		X			X			Al, Cu, Ag, Au	100 - 1200
(Kerrick et al. 1973)	X					X[1]		C	40 - 170
(Jurek et al. 1994)	X						X	C, Au	50 - 85
(Bastin & Heijligers 2000a)			X	X				Al	10 - 320
(Bastin & Heijligers 2000b)	X		X			X[2]		Pd	10 - 320
(Campos et al. 2001)	X		X					Al, Ti, Cr, Cu, Nb, Mo, Au	30 - 440
(Statham et al. 2012)				X				Al – Pd**	10 - 320

*QCM – Quartz Crystal Microbalance; OI – Optical Interferometry; RBS – Rutherford Backscattering; MC – Monte Carlo; Grav. – Gravimetry; Opt. – Optical ([1]colour change or [2]cross-section); XRR – X-Ray Reflectometry.
**Used Bastin & Heijligers(Bastin & Heijligers 2000a; Bastin & Heijligers 2000b) databases of measurements.

Table 1 Compilation of the measurement methods used, coating elements and thickness ranges for studies previously carried out to determine the accuracies of film thickness determinations.

RBS is reported to provide the only truly independent measure of the film thickness (Bastin & Heijligers 2000a). However, requiring a particle accelerator, it is not readily accessible. Furthermore, this method is not accurate for coatings less than about 20nm, and cannot resolve near-neighbour elemental components (Limandri et al. 2010). The majority of vacuum and sputter coaters, where they provide thickness measurement, have film thickness monitors based on the QCM. These are frequently the only measurement made of the thicknesses of deposited films. Whilst these can measure thicknesses to Angstrom precisions, for accurate absolute measurements these must be calibrated against another technique (Bastin & Heijligers 2000b; Campos et al. 2001). Jurek et al, in their 1994 study, stated that *"Unfortunately, the accurate measurement of the mass thickness is not trivial in spite of the fact that many evaporators are equipped by mass thickness monitors; they never can be placed exactly at the same place on the specimen and also their accurate calibration is rather problematic"* (Jurek et al. 1994). Consequently the accuracy of the thickness values derived is seldom known. For conventional high accelerating voltage (15-20 kV) analyses this is normally not an issue, but at low voltage or low overvoltage conditions, an accurate knowledge of the coating thickness becomes more critical.

In this study a comparison is made between FIB measurements, FTM measurements and calculated thicknesses derived from fitting EPMA experimental measurements to $\phi(\rho z)$ and Monte Carlo calculations for Al and Cu coatings on bulk Bi samples. The effect of errors in coat thickness measurements on the quantification of the substrate is also investigated.

The samples reported in this study are a subset of a wider range of coatings. Al and Cu proved to be the simplest to model of all the coating materials investigated. For example, C was found to exhibit both deposition and erosion during analysis, and will be reported separately. Both Cu and Al have been favoured as coating materials in the past (Yakowitz 1968; Bottomley et al. 2000): Al has a lower mass attenuation coefficient than C at energies

below ~1.5 keV (Love et al. 1974; Bastin & Heijligers 1991), whilst Cu has superior electrical and thermal conductivity than either C or Al (Yakowitz 1968).

Bi is being used by the authors as a heavy metal surrogate for actinide elements, which are both difficult to obtain as high purity bulk samples, and require special handling and preparation owing to their toxicity and radioactivity (Walker 1999). However, the restrictions of low voltage analyses commonly requires the use of low energy L or M lines and the results presented here are therefore more generally applicable.

Materials and Methods

To test both the accuracy and repeatability of coatings measured with a quartz crystal microbalance FTM, polished samples of Bi metal were Ar plasma sputter coated with a range of thicknesses of Al and Cu. For each sample a fixed 5nm target thickness was set and nominal thicknesses of 5, 10, 15 and 20 nm coatings deposited by applying 1, 2, 3 or 4, '5nm' coatings. In the following text these nominal values will be denoted in single quotes to differentiate them from measured or calculated thicknesses. The repeatability of the FTM could thus be tested by checking the linearity of the increase in total thickness across the four samples. Using a fixed coating thickness, and therefore similar coating time for each interval, also minimises any differences in response of the FTM sensor due to different levels of heating between the different final target thicknesses. Without any prior knowledge of the true coating density the bulk elemental Al and Cu values, 2.70gcm^{-3} and 8.96 gcm^{-3} respectively, were assumed for the FTM settings. For the Cu coatings a Leica ACE EM 600 coater was used. This model co-locates the FTM sensor with the samples being coated. An ultimate chamber vacuum of 5x10^{-4} Pa was reached before bleeding Ar gas in to a level of 8x10^{-1} Pa for coating. The Quorum Q150TS coater used for the Al coatings has a more conventional FTM sensor placement to one side of the sample platen. The ultimate vacuum, at 5x10^{-3} Pa, was slightly poorer than for the Leica coater, but the Ar pressure was the same for coating. The difference in distance of the FTM sensor and the sample from the coating source for the Q150TS was compensated for using a tooling factor of 2.0. Both coaters were purged with Ar, and a mechanical shutter shielded the coating source for the initial few seconds of sputtering to allow any surface oxide to be removed and the source to fully stabilise.

K-ratios for Al Kα, Cu Lα and Bi Mα were measured using a JEOL JXA-8530F EPMA at 5, 7, 10 and 15 kV, with a beam current of 25 nA, defocussed to a 10 μm diameter, and count times of 60s on peak and 30s on each of two backgrounds. Uncoated pure Al, Cu and Bi metal were used as standards. 12 analysis points were acquired for each coating thickness, at each accelerating voltage. Immediately prior to analysis the reference materials were polished to 1 μm diamond under oil, washed with isopropanol and rinsed with ethanol. The derived k-ratios were converted directly into modelled film thicknesses using GMRFilm (Waldo 1988), and indirectly using empirical film thickness versus k-ratio relationships derived using both DTSA-II (Ritchie et al. 2008) and the PENEPMA variant of PENELOPE (Salvat 2015; Llovet & Salvat 2016). Film thickness versus k-ratio correlations were also generated with GMRFilm to allow the results from the three software packages to be more directly compared to each other. K-ratio values were calculated directly by GMRFilm, but this is not possible using DTSA-II or PENEPMA. Instead, for these latter two, emitted intensities were calculated for both pure Al, Cu and Bi metal as bulk samples and coated Bi as layered samples, the bulk samples acting as pure reference materials. The k-ratio was calculated by dividing the

calculated layered sample intensity value by the bulk intensity for each film thickness, at each accelerating voltage.

GMRFilm uses an iterative calculation algorithm, whereas both DTSA-II and PENEPMA are Monte Carlo routines which differ in the degree of fidelity (and consequently computer processing time) used to model the electron-photon interactions in the sample. For example, DTSA-II uses tabulated sets of correction factors, such as the Mass Attenuation Coefficients (MAC) and the ionisation cross-sections, whilst PENELOPE/PENEPMA uses calculated or modelled probabilities for each possible interaction event. All three packages allow for the correction of secondary fluorescence to be included. For each of the three software packages the key settings applied are summarised in Table 2. Unless otherwise stated the default settings were used for each package. The Al and Cu film densities used in all cases were 2.70 gcm^{-3} and 8.96 gcm^{-3} respectively.

GMRFilm	• Version: 05/1993 • Iterations: max. 15 • $\phi(\rho z)$: Pouchou and Pichoir PAP, Scanning (1990) • MAC's: Heinrich IXCOM-11 • Fluorescence: Yes
DTSA-II	• Version: Iona (08/2015) • $\phi(\rho z)$: Pouchou and Pichoir XPP • MAC's: Heinrich IXCOM-11 • Ionisation cross-sections: Bote/Salvat 2008 • Probe dose: 600nAs • Fluorescence: Yes

PENEPMA*	• Version: 2014
	• Trajectories: $1x10^7$
	• Fluorescence: Yes
	• C_1: 0 (coat), 0.2 (substrate)
	• C_2: 0 (coat), 0.2 (substrate)
	• W_{cc}: 0 (coat), 1e3 (substrate)
	• W_{cr}: -10 (coat), 1e3 (substrate)
	• S_{max} (film): $1/10^{th}$ coating thickness
	• Variance reduction: Yes
	  ○ Forcing: Yes
	  ○ Splitting: No

Table 2 Key values and settings used for the modelling programs DTSA-II, GMRFilm, and PENEPMA. See Salvat 2015 and Salvat and Llovet 2016 for descriptions of the PENELOPE/PENEPMA parameters.*

Results

Cu coating on Bi

The measured Cu Lα and Bi Mα k-ratio values, at each accelerating voltage, for the four Bi samples with '5', '10', '15' and '20 nm' Cu coating thicknesses respectively, are given in Table 3 and plotted in Figure 2.

		Cu Lα		Bi Mα	
kV	**FTM (nm)**	**Mean**	*Std. Dev.*	**Mean**	*Std. Dev.*
5	**5.46**	0.1155	*0.0018*	0.8569	*0.0056*
	10.96	0.2372	*0.0022*	0.7150	*0.0055*
	16.43	0.3570	*0.0035*	0.5556	*0.0093*
	21.92	0.4435	*0.0043*	0.4494	*0.0090*
7	**5.46**	0.0647	*0.0008*	0.9268	*0.0106*
	10.96	0.1348	*0.0011*	0.8593	*0.0111*
	16.43	0.2099	*0.0013*	0.7698	*0.0122*
	21.92	0.2698	*0.0023*	0.7028	*0.0148*
10	**5.46**	0.0364	*0.0006*	0.9709	*0.0032*
	10.96	0.0750	*0.0009*	0.9382	*0.0044*
	16.43	0.1174	*0.0013*	0.8944	*0.0031*
	21.92	0.1517	*0.0019*	0.8617	*0.0034*
15	**5.46**	0.0215	*0.0003*	0.9808	*0.0025*
	10.96	0.0434	*0.0004*	0.9632	*0.0020*
	16.43	0.0671	*0.0007*	0.9384	*0.0041*
	21.92	0.0865	*0.0011*	0.9272	*0.0040*

Table 3 Measured K-ratios for Cu Lα and Bi Mα for each of the four Cu coated Bi samples at each of the four accelerating voltages. Mean and standard deviation values are derived from 12 analyses for each sample.

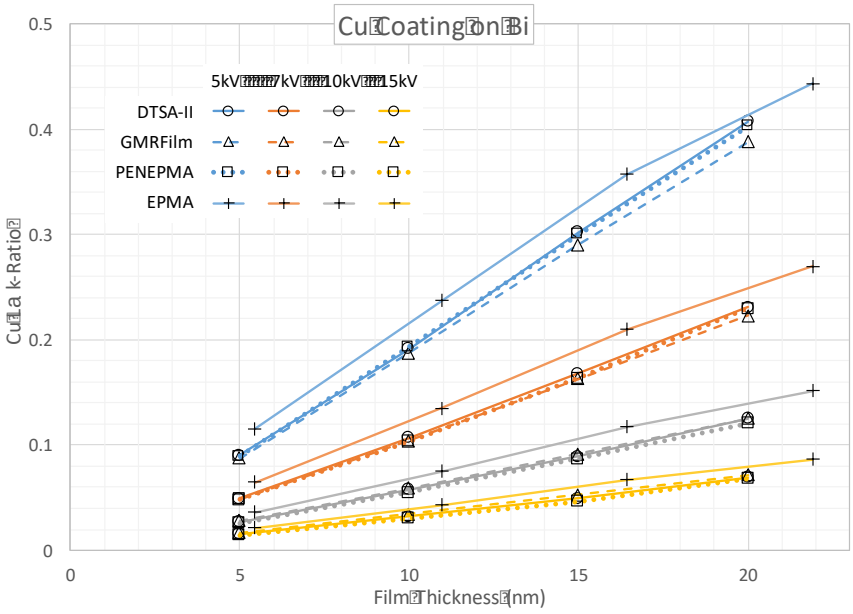

Figure 2 Plot of Cu Lα k-ratio values calculated using DTSA-II (circles and solid lines), GMR-Film (triangles and dashed lines) and PENEPMA (squares and dotted lines), and measured by EPMA (crosses and solid lines) as functions of accelerating voltage and coating thickness for a Cu film on a Bi substrate. EPMA values are plotted using the FTM thicknesses.

Calculated Cu Lα k-ratios for 5, 10, 15 and 20nm coatings on Bi are summarised in Table 4 and Figure 2. These show that the three models for calculating k-ratios are in relatively good

agreement with each other, although the maximum difference of ~10% is not insignificant. This occurs where we would expect the film correction to be largest, i.e. at the lowest accelerating voltage and greatest coating thickness modelled, 5kV and 20nm. At these conditions DTSA-II produces a k-ratio value of 0.42 and GMRFilm one of 0.39. The plots also show that, over the modest range of thicknesses modelled, the calculated k-ratios can be closely approximated as linear functions of coating thickness at each accelerating voltage. The linear coefficients, m and c, and the R^2 fit values are also given in Table 4. The R^2 values show that the linear functions are extremely good approximations of the correlations. Being able to approximate the relationship using a linear function has the benefit that the correlation can be derived by relatively few points, and any measured k-ratio values can be easily converted into coating thickness. It is also evident from Figure 2 that the calculated k-ratio values do not match the measured k-ratios at the FTM thicknesses.

		Cu Lα k-ratio Coating Thickness (nm)				**Linear Coefficients** *(k-ratio=***m***.thickness+***c***)*		
kV	**Software**	**5**	**10**	**15**	**20**	**m**	**c**	**R^2**
5	DTSA-II	0.0927	0.2046	0.2968	0.4193	0.0214	-0.0147	0.9973
	PENEPMA	0.0896	0.1934	0.3003	0.4028	0.0209	-0.0151	0.9999
	GMRFilm	0.0875	0.1878	0.2905	0.3878	0.0201	-0.0125	0.9999
7	DTSA-II	0.0509	0.1089	0.1683	0.2263	0.0117	-0.0079	1.000
	PENEPMA	0.0484	0.1037	0.1633	0.2297	0.0121	-0.0146	0.9983
	GMRFilm	0.0491	0.1041	0.1628	0.2231	0.0116	-0.0104	0.9996
10	DTSA-II	0.0279	0.0585	0.0885	0.1246	0.0064	-0.0052	0.9980
	PENEPMA	0.0261	0.0552	0.0871	0.1209	0.0063	-0.0068	0.9989
	GMRFilm	0.0283	0.0590	0.0914	0.1252	0.0065	-0.0048	0.9995
15	DTSA-II	0.0154	0.0305	0.0506	0.0693	0.0036	-0.0040	0.9969
	PENEPMA	0.0145	0.0306	0.0465	0.0680	0.0035	-0.0042	0.9944
	GMRFilm	0.0168	0.0344	0.0526	0.0714	0.0036	-0.0017	0.9998

Table 4 Emitted Cu Lα k-ratio values calculated using DTSA-II, PENEPMA and GMR-Film, as functions of accelerating voltage and coating thickness for a Cu film on a Bi substrates, and linear coefficients and R^2 fit values for the k-ratios as functions of the film thickness at the four accelerating voltages.

Using the derived linear correlations for DTSA-II and PENEPMA, the measured Cu Lα k-ratio values were converted into film thickness values. For GMRFilm the film thicknesses were calculated directly from the measured k-ratio values. The resulting thicknesses and their percentage differences from the FTM values are plotted in Figure 3. From Figure 3a) we can see that each set of data produces a linear increase in thickness across the four samples. From Figure 3b) we can see that all samples produced thicker values relative to the FTM, with relative differences ranging from +8% to +23%. All three calculated data sets show increased disparity to FTM with decreasing film thickness. The differences between the calculation methods also increases with decreasing film thickness. However, the differences between the calculated values is significantly less than the differences between these and the FTM values. Both GMRFilm and DTSA-II show good agreement with the single FIB data point.

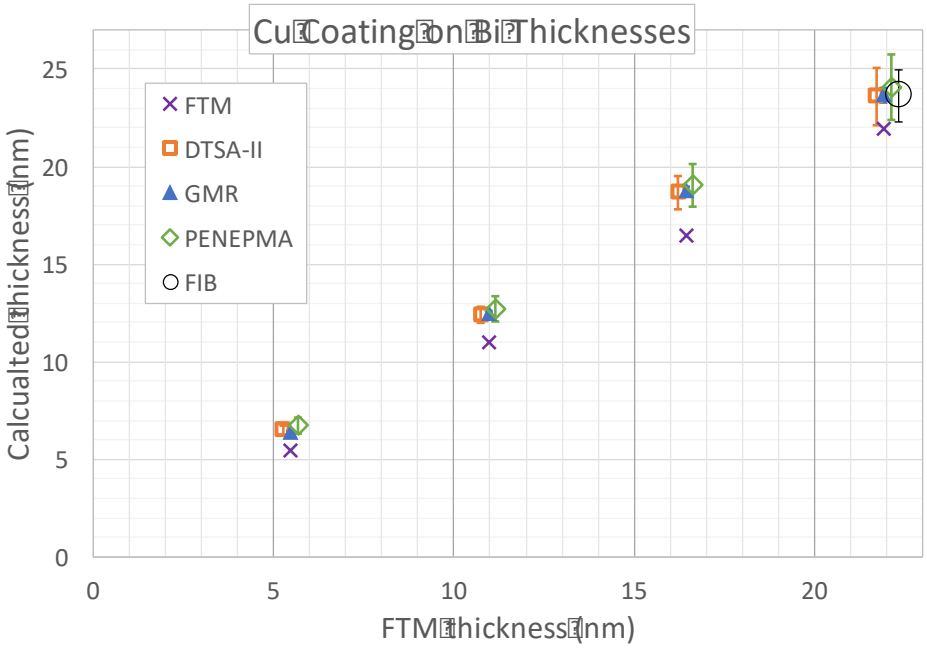

a)

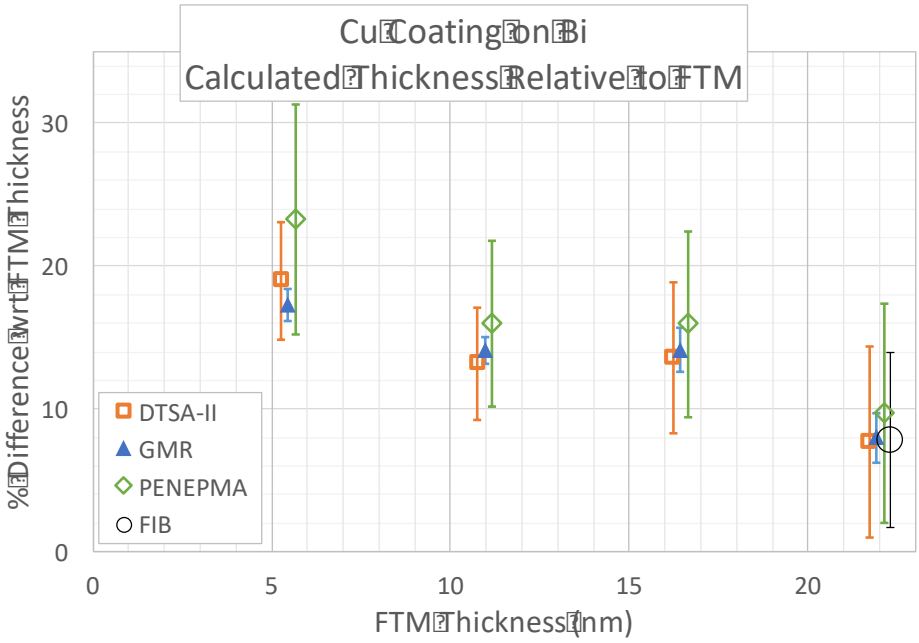

b)

Figure 3 Comparison of the calculated Cu coatings on Bi from DTSA-II, GMRFilm, and PENEPMA, and measured by FIB sectioning, a) relative to the FTM thicknesses, and b) as percentage differences from the FTM thicknesses. The calculated values are the means of the thicknesses calculated at all four accelerating voltages for each data set. The FIB data point is the mean of 10 measurements. Note that a small x-axis offset has been applied to allow the error bars to be more easily seen.

Al coating on Bi

The means and standard deviations of the 12 EPMA measured Al Kα and Bi Mα k-ratio values measured for each sample, at each accelerating voltage, are given in Table 5 and plotted in Figure 4.

		Al Kα		Bi Mα	
kV	**FTM (nm)**	**Mean**	*Std. Dev.*	**Mean**	*Std. Dev.*
5	**4.4**	0.0721	*0.0071*	0.8933	*0.0176*
	8.6	0.1517	*0.0348*	0.7340	*0.0919*
	13.1	0.2224	*0.0042*	0.6802	*0.0199*
	18.3	0.3032	*0.0109*	0.5335	*0.0291*
7	**4.4**	0.0432	*0.0142*	0.9376	*0.0310*
	8.6	0.0723	*0.0029*	0.9054	*0.0064*
	13.1	0.1192	*0.0023*	0.8525	*0.0226*
	18.3	0.1712	*0.0048*	0.7806	*0.0182*
10	**4.4**	0.0204	*0.0024*	0.9731	*0.0099*
	8.6	0.0370	*0.0028*	0.9641	*0.0059*
	13.1	0.0619	*0.0023*	0.9281	*0.0203*
	18.3	0.0877	*0.0030*	0.9064	*0.0064*
15	**4.4**	0.0108	*0.0026*	0.9843	*0.0060*
	8.6	0.0177	*0.0008*	0.9788	*0.0037*
	13.1	0.0302	*0.0013*	0.9578	*0.0075*
	18.3	0.0438	*0.0026*	0.9459	*0.0058*

Table 5 Mean and standard deviation values for the 12 EPMA measured k-ratios for Al Kα and Bi Mα measured for each of the four coated samples at each of the four accelerating voltages.

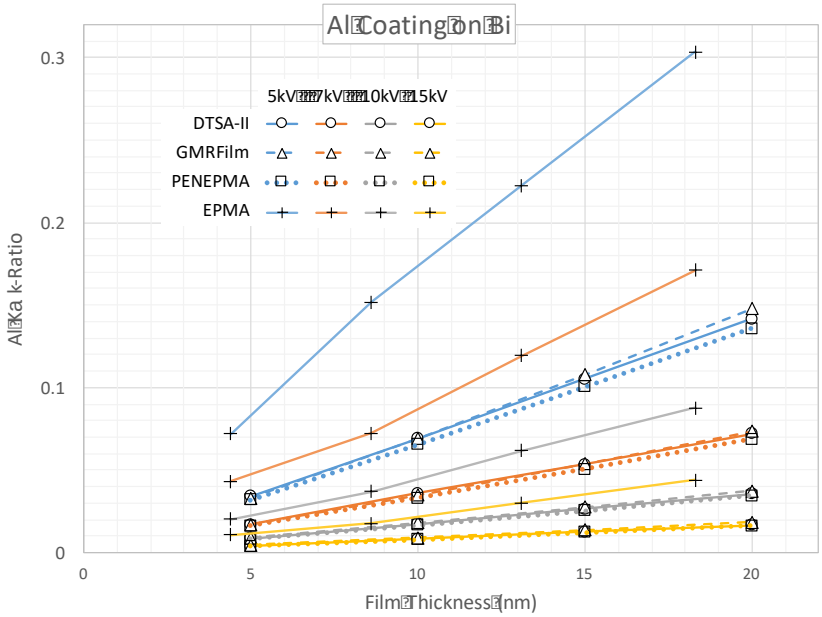

Figure 4 Plot of emitted Al Kα k-ratio values calculated using DTSA-II, GMR-Film and PENEPMA, and measured by EPMA as functions of accelerating voltage and coating thickness for a Al film on a Bi substrate. EPMA values are plotted using the FTM thicknesses.

The calculated emitted Al Kα k-ratios are summarised in Table 6 and Figure 4. These show that, as for the Cu on Bi samples, the three sets of values are in relatively good agreement, differing by a maximum of ~9% at 5kV and 20nm. At these conditions PENEPMA produces a k-ratio of 0.136 and GMRFilm one of 0.148. Again, the R^2 linear fit values in Table 6 show that, over the range of thicknesses modelled, the calculated k-ratios at each accelerating voltage can be closely approximated as linear functions of coating thickness.

Calculated film thicknesses, derived in the same way as for the Cu on Bi sample, are plotted in Figure 5a), and as percent differences from the FTM values in Figure 5b). The software calculated film thicknesses agree relatively well with each other, but differ substantially from the FTM values, being ~1.5x greater than the FTM values. Unlike for the Cu on Bi samples, where there was some agreement between the FIB and calculated thicknesses, the measured thicknesses from FIB cross-sections of two of the Al on Bi samples exceed both the software calculations and FTM measurements: The nominally 20 nm coating was measured at over 60 nm, more than 3x greater than the FTM indicated thickness.

		Al Kα k-ratio Coating Thickness (nm)				**Linear Coefficients** *(k-ratio=***m***.thickness+***c***)**		
kV	**Software**	**5**	**10**	**15**	**20**	**m**	**c**	**R^2**
5	DTSA-II	0.0334	0.0678	0.1028	0.1388	0.0070	-0.0021	0.9999
	PENEPMA	0.0319	0.0655	0.1003	0.1359	0.0069	-0.0033	0.9998
	GMRFilm	0.0330	0.0692	0.1078	0.1478	0.0077	-0.0063	0.9995
7	DTSA-II	0.0171	0.0349	0.0548	0.0737	0.0038	-0.0023	0.9995
	PENEPMA	0.0162	0.0332	0.0507	0.0687	0.0035	-0.0016	0.9998
	GMRFilm	0.0170	0.0351	0.0539	0.0736	0.0038	-0.0022	0.9996
10	DTSA-II	0.0086	0.0167	0.0271	0.0353	0.0018	-0.0007	0.9977
	PENEPMA	0.0082	0.0166	0.0254	0.0343	0.0018	-0.0007	0.9999
	GMRFilm	0.0089	0.0181	0.0275	0.0373	0.0019	-0.0007	0.9998
15	DTSA-II	0.0041	0.0087	0.0124	0.0171	0.0009	-0.0001	0.9975
	PENEPMA	0.0039	0.0080	0.0122	0.0164	0.0008	-0.0003	0.9999
	GMRFilm	0.0045	0.0090	0.0137	0.0184	0.0009	-0.0002	0.9999

Table 6 Emitted Al Kα k-ratio values calculated using DTSA-II, PENEPMA and GMR-Film, as functions of accelerating voltage and coating thickness for a Al film on a Bi substrates, and linear coefficients and R^2 fit values for the k-ratios as functions of the film thickness at the four accelerating voltages.

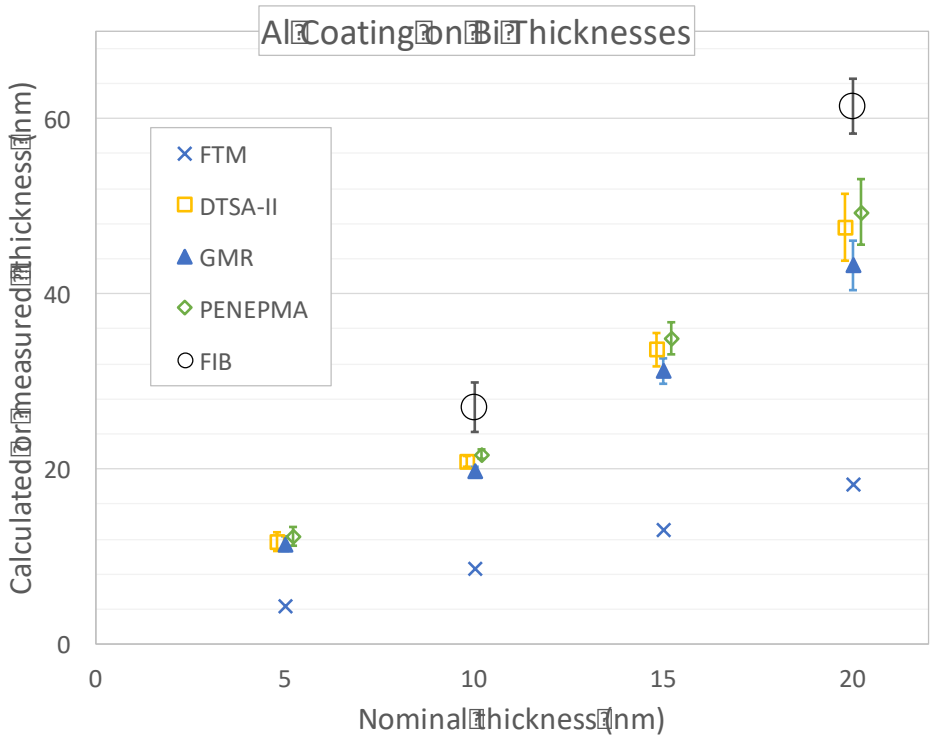

a)

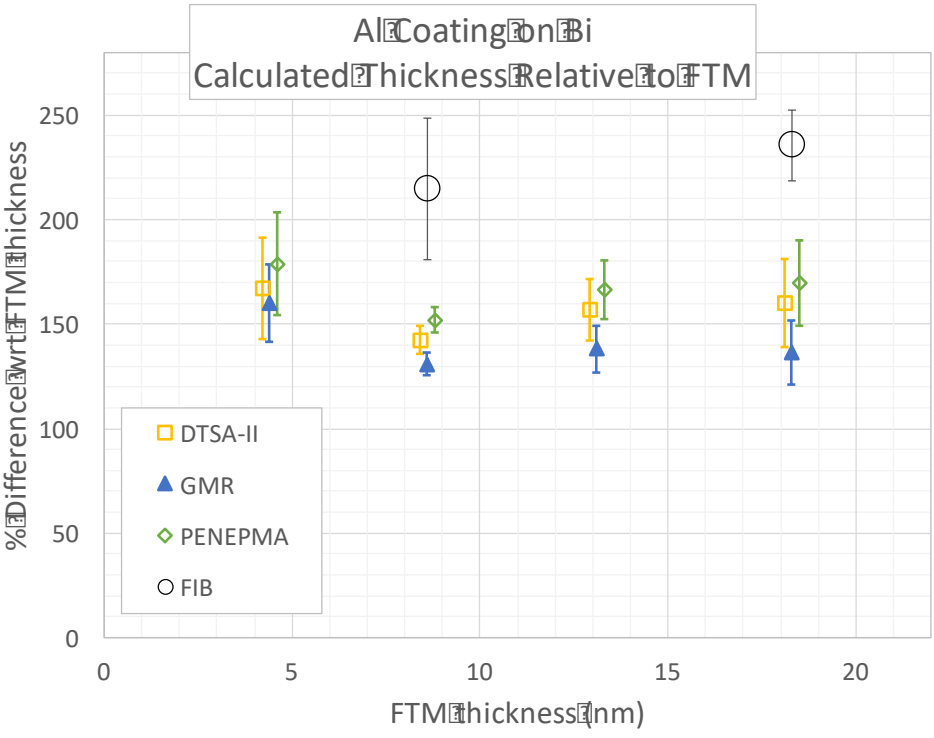

b)

Figure 5 Comparison of the calculated Al coatings on Bi from DTSA-II, GMRFilm, and PENEPMA, and measured by FIB sectioning, a) relative to the nominal thicknesses, and b) as percentage differences from the FTM thicknesses. The calculated values are the means of the thicknesses calculated at all four accelerating voltages for each data set. The FIB data points are the means of 18 ('10 nm' coating) and 8 ('20 nm' coating) measurements. Note that a small x-axis offset has been applied to allow the error bars to be more easily seen.

Despite the very large differences between the calculated, FIB and FTM datasets, the relative changes in film thicknesses between each set of four samples all show linear trends, indicating that at least the repeatability of the coating depositions has been good.

Substrate Quantification

When quantifying a sample which either differs from a standard in coating thickness, or where either the standard or unknown is uncoated, the intensity can be corrected using the measured coating thickness. However, any uncertainty or error in the coating thickness will be propagated on to quantification of the substrate. For these samples the substrate is pure Bi. The analytical error for substrate quantification is determined from the ratio of the calculated to the measured Bi Mα k-ratios.

The calculated Bi Mα k-ratios, like the film k-ratios, show strongly linear trends against coat thickness, over the range considered. Table 7 and Table 8 show both the linear coefficients and the R^2 values at each of the four accelerating voltages for the Cu on Bi and Al on Bi systems respectively.

Bi Mα linear coefficients for Cu on Bi Samples
*(k-ratio=***m.***Cu-thickness+***c)*

	PENEPMA			DTSA-II			GMRFilm		
kV	**m**	**c**	**R^2**	**m**	**c**	**R^2**	**m**	**c**	**R^2**
5	-0.0242	1.0275	0.9995	-0.0252	1.0178	0.9994	-0.0241	0.9900	0.9972
7	-0.0114	1.0127	0.9993	-0.0120	1.0159	0.9981	-0.0141	1.0107	0.9999
10	-0.0057	1.0066	0.9958	-0.0061	1.0070	0.9856	-0.0073	1.0051	0.9997
15	-0.0031	1.0049	0.9909	-0.0031	1.0081	0.9619	-0.0039	1.0012	0.9999

Table 7 PENEPMA, DTSA-II and GMRFilm calculated linear coefficients and R^2 goodness of fit values for emitted Bi Mα k-ratio as a function of Cu coating thickness in the range 5 – 20 nm.

Bi Mα linear coefficients for Al on Bi Samples
*(k-ratio=***m.***Al-thickness+***c)*

	PENEPMA			DTSA-II			GMRFilm		
kV	**m**	**c**	**R^2**	**m**	**c**	**R^2**	**m**	**c**	**R^2**
5	-0.0067	1.0141	0.9983	-0.0067	0.9971	0.9993	-0.0092	1.0073	0.9997
7	-0.0028	1.0007	0.9865	-0.0030	1.0076	0.8766	-0.0044	1.0028	0.9996
10	-0.0014	0.9999	0.9733	-0.0013	0.9911	0.7184	-0.0023	1.0008	0.9999
15	-0.0009	1.0009	0.9173	-0.0015	1.0156	0.9756	-0.0013	1.0002	1.0000

Table 8 PENEPMA, DTSA-II and GMRFilm calculated linear coefficients and R^2 goodness of fit values for emitted Bi Mα k-ratio as a function of Al coating thickness in the range 5 – 20 nm.

Bi Mα k-ratio values, were calculated for the samples representing the extremes in coat thickness using the FTM, FIB and EPMA thicknesses. The values calculated from all three software packages are compared against the EPMA values for the Cu and Al coated samples in Figure 6 and Figure 7 respectively.

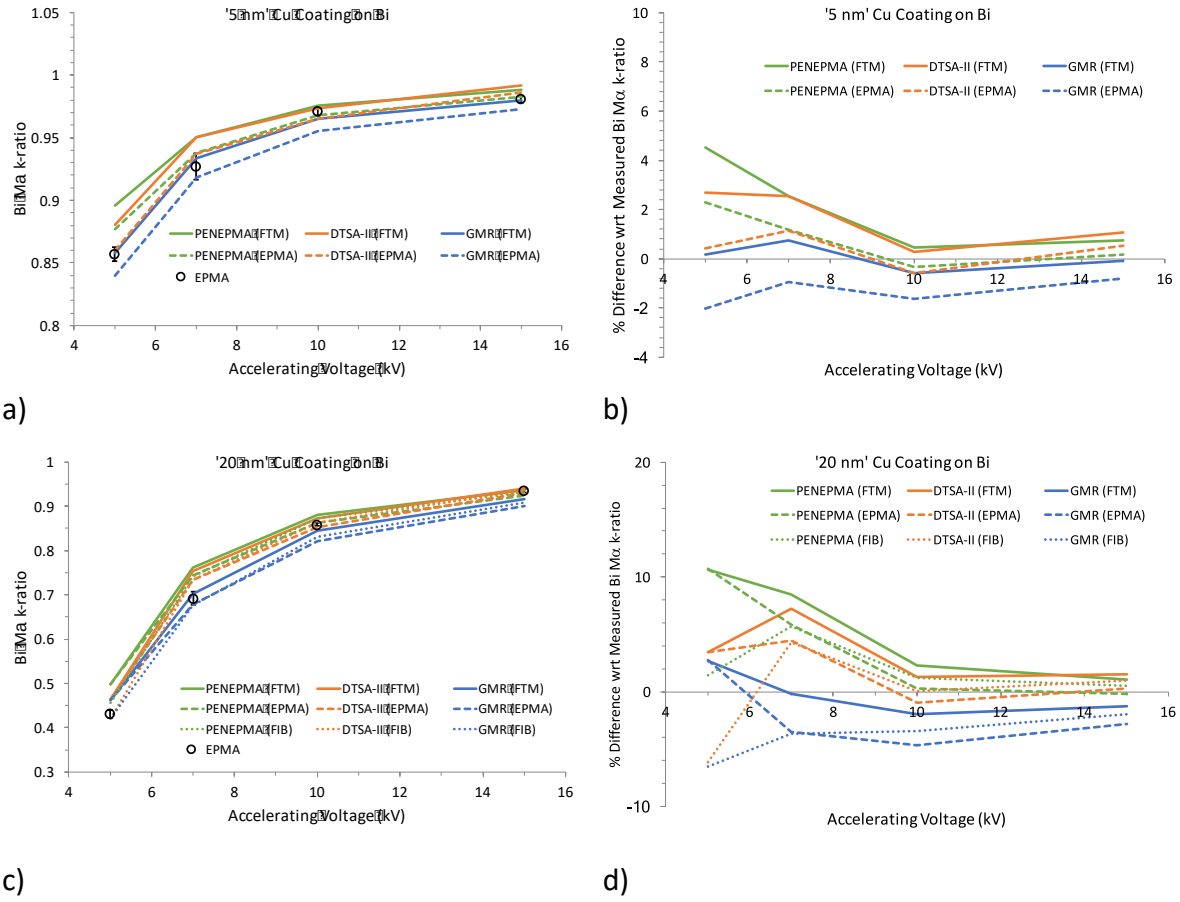

Figure 6 Comparisons of calculated Bi Mα k-ratios for the thinnest (a and b) and thickest (c and d) Cu on Bi samples against the EPMA experimentally measured values in absolute values (a and c) and percent differences (b and d). In each plot k-ratios have been calculated using PENEPMA (green lines), DTSA-II (orange lines), and GMRFilm (blue lines) assuming coating thicknesses given by FTM (solid lines) and calculated by PENEPMA, DTSA-II and GMRFilm from the EPMA measured coating k-ratios (dashed lines).The thickest coated sample also includes k-ratios calculated using the FIB measured film thicknesses (dotted lines).

For the Cu on Bi samples, where the FTM thicknesses and those calculated from the EPMA measured Cu k-ratios agreed to within ~10 – 20%, each 'FTM' and 'EPMA' pair of calculated Bi Mα k-ratios differs by only ~1% at 15kV for the thinnest coating (Figure 6b)), increasing to ~4% at 5 kV for the thickest sample (Figure 6d). The total range of errors similarly increases from ~±1% to ~±10%. At 10kV and 15 kV the PENEPMA calculated Bi k-ratios using the EPMA derived thicknesses produces the closest values to the EPMA measurements, although DTSA-II using EPMA thicknesses and GMRFilm using the FTM values are also close. Below 10kV the GMRFilm with FTM combination produces the smallest errors. The calculated k-ratios using the FIB measured thicknesses for the '20 nm' sample, which are plotted in Figure 6d), show similar error ranges to those calculated from the EPMA and FTM thicknesses. Overall, the GMRFilm and FTM combination produces the most consistent results, with errors of ~±2% under most of the modelled conditions.

For the Al on Bi samples, where there are significant differences in the coating thickness values given by the FTM and those calculated from the EPMA coating k-ratios, the discrepancies between the calculated and measured Bi Mα k-ratios are more significant and the trends more consistent between the datasets: The EPMA-derived coating thicknesses provide significantly closer Bi Mα k-ratios than the FTM values at all accelerating voltages. The overestimations still increase with decreasing accelerating voltage: The EPMA-derived

thickness data shows errors increasing from ~2% for the ‘5 nm’ sample at 15 kV (Figure 7b)), to 20 – 35% for the ’20 nm’ sample at 5kV. The FTM based results, however, show very large errors, increasing to a 70 - 80% overestimation of the Bi Mα k-ratio at 5kV from both GMRFilm and PENEPMA. The FIB derived k-ratios for the ’20 nm’ sample (Figure 7d)) only produce the best results at 5 kV, but still have errors of ~±20%.

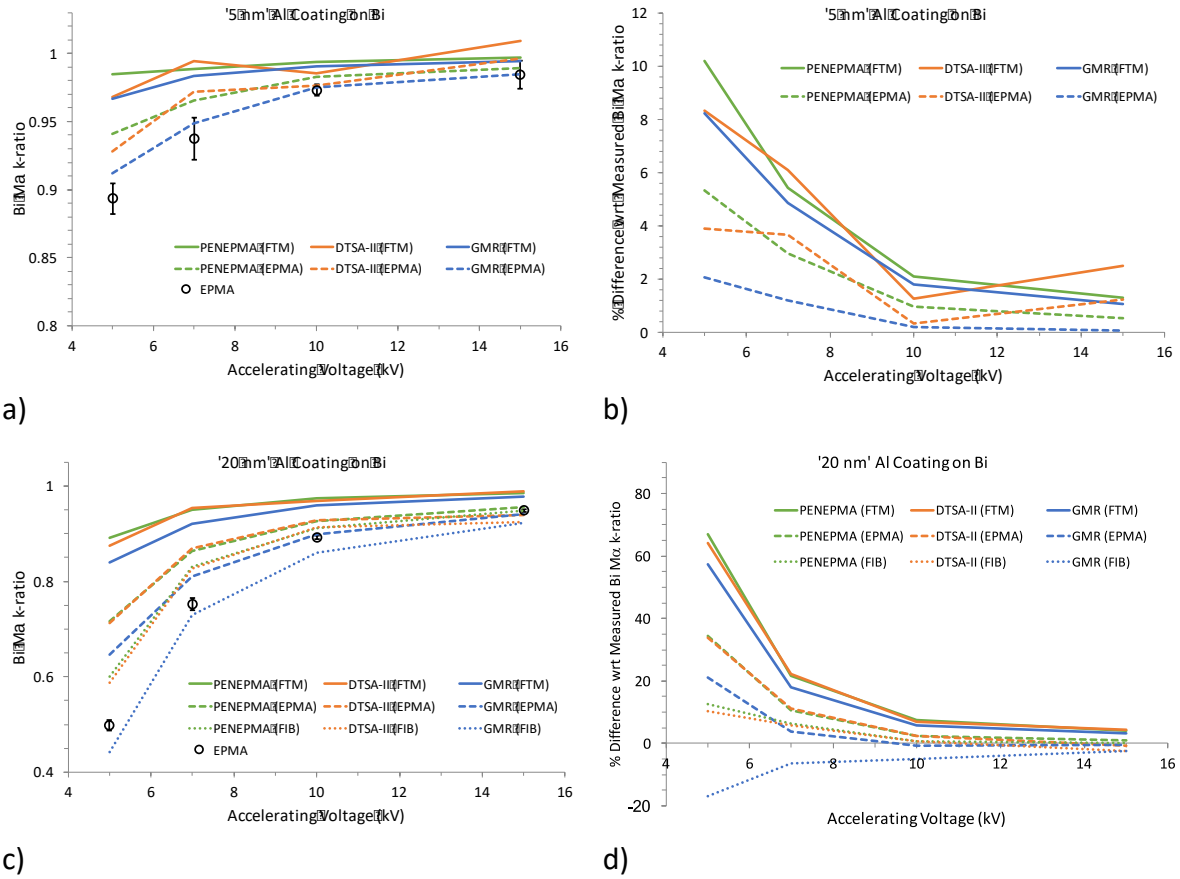

Figure 7 Comparisons of calculated Bi Mα k-ratios for the thinnest (a and b) and thickest (c and d) Al on Bi samples against the EPMA experimentally measured values in absolute values (a and c) and percent differences (b and d). In each plot k-ratios have been calculated using PENEPMA (green lines), DTSA-II (orange lines), and GMRFilm (blue lines) assuming coating thicknesses given by FTM (solid lines) and calculated by PENEPMA, DTSA-II and GMRFilm from the EPMA measured coating k-ratios (dashed lines). The thickest coated sample also includes k-ratios calculated using the FIB measured film thicknesses (dotted lines).

Discussion

Al on Bi

It is apparent from the Al on Bi results that huge discrepancies are possible for both the coating thickness determination and, as a result, substrate quantification: Under the least favourable conditions modelled, for a thick coating at 5 kV, the experimentally measured coating thickness differs from the FTM value by a factor of 3, propagating to an overestimation of the substrate k-ratio by 70%. This would subsequently produce a commensurate under-measurement of the substrate composition. With these magnitudes of errors quantification would be largely meaningless. The differences can be attributed to several factors, for example the FTM tooling factor, the assumed Al density, and the extrapolation of the thickness versus k-ratio relationship. It is possible, although we believe

unlikely, that despite the relatively high ultimate vacuum level and the Ar purging, the Al has absorbed some residual oxygen during the coating procedure. However, there was no discernible Al_2O_3 precipitation in the FIB sections and, since the oxide has a higher density than the metal (3.95 gcm^{-3} compared to 2.70 gcm^{-3}), dissolved oxygen would be expected to reduce rather than increase the thickness of the coating.

The FIB and calculated values fall well beyond the modelled thickness range so extrapolation errors could account for at least some of the discrepancies between these and the FTM values. Additional k-ratio vs Al film thickness correlations were therefore calculated at 30, 50, 70 and 100 nm. Figure 8 shows that the 5 – 20 nm calculated linear trends, unsurprisingly, become more inaccurate the further they are extended beyond 20 nm. However, the fits are still reasonable up to ~60 nm and are at least sufficient to show that this factor can't account for more than a minor portion of the very large discrepancy between the calculated and FTM thicknesses.

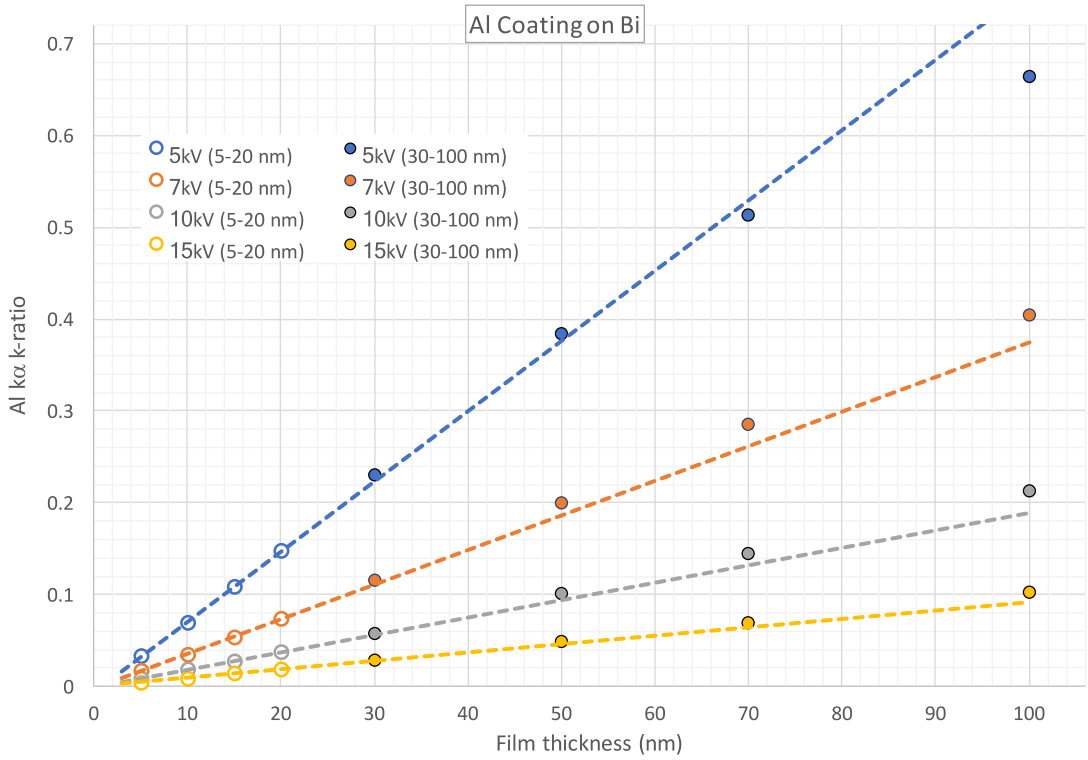

Figure 8 K-ratio versus Al film thickness correlations for 5 – 20 nm (open circles) and 30 – 100 nm (closed circles) film thickness ranges calculated using GMRFilm. The dashed lines are the linear trends extrapolated from the 5 – 20 nm data points.

The ~30% difference between the FIB measured thicknesses and those calculated from the EPMA measured Al k-ratios (Figure 5b) can logically be attributed to the film density: Since the FIB values are direct measurements of the geometric thickness whilst the calculated values are mass thickness values, this difference can be corrected for by using a lower than bulk density for the Al. Previous studies have identified that thin films can exhibit significantly lower densities. For example, using the lowest Al density, ~2 gcm^{-3}, that Hartman (1965) measured for his thinnest film (~25 nm) brings the software calculated thicknesses into closer agreement with the FIB section values, as is shown in Figure 9 and Table 9: The relative differences between the software calculated thicknesses and the FIB measured values is reduced to <10%.

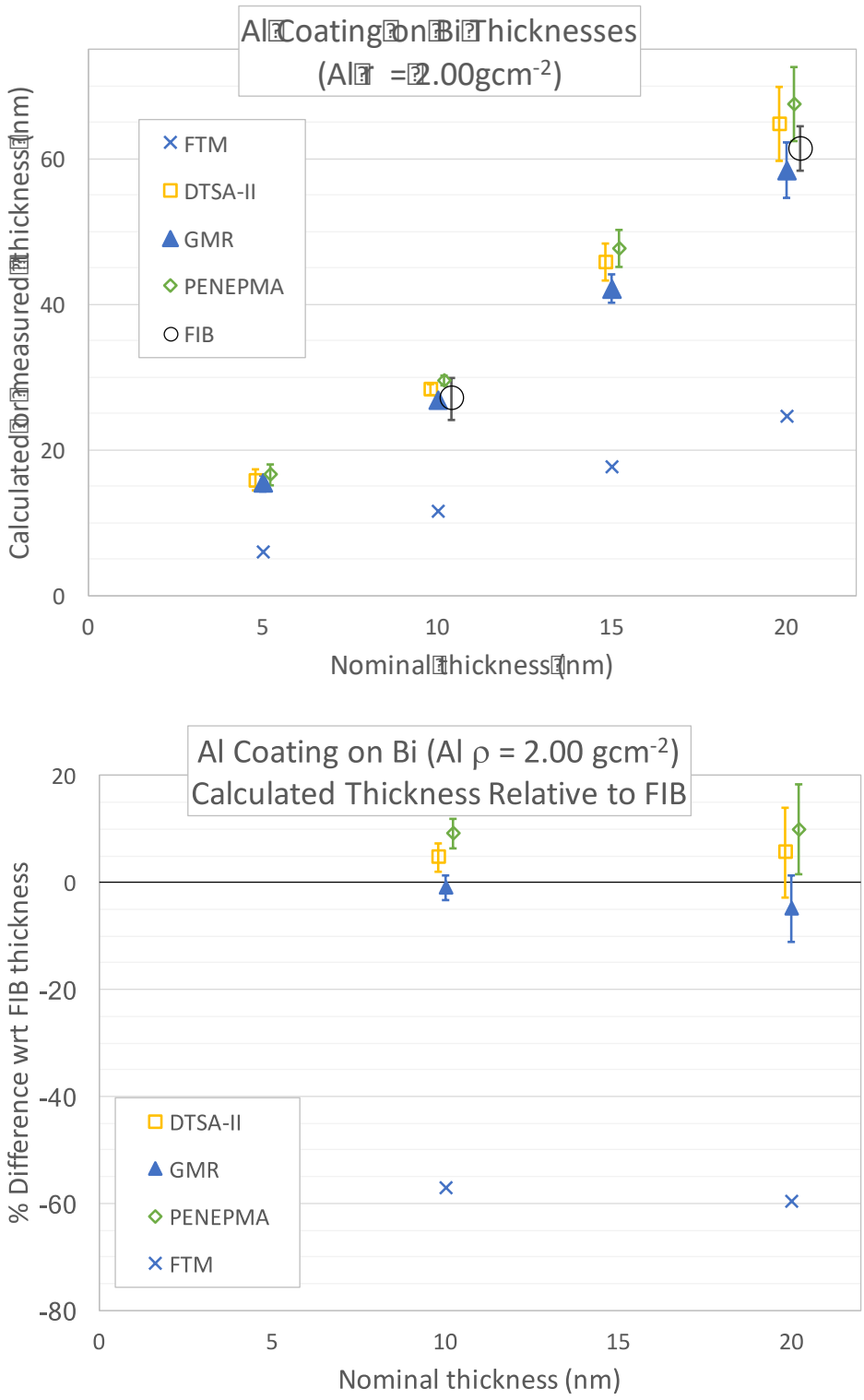

Figure 9 Comparison of the re-calculated Al coatings on Bi from DTSA-II, GMRFilm, PENEPMA and FTM using an Al density of 2.00 gcm^{-2}, and measured by FIB sectioning, a) as absolute values, and b) as percentage differences from the FIB thicknesses. Note that a small x-axis offset has been applied to allow the error bars to be more easily seen.

		Coating Thickness (nm) FIB Thickness (nm)				% Difference wrt FIB FIB Thickness (nm)			
ρ (gcm^{-3})	**Software**	**(12.19)**	**27.06**	**(42.99)**	**61.40**	**(12.19)**	**27.06**	**(42.99)**	**61.40**
2.70	FTM	4.4	8.6	13.1	18.3	-	-68.21	-	-70.20
	DTSA-II	11.75	20.82	33.64	47.59	-	-22.94	-	-22.49
	PENEPMA	12.27	21.67	34.90	49.31	-	-19.89	-	-19.68
	GMRFilm	11.44	19.85	31.21	43.27	-	-26.64	-	-29.53
2.00	FTM	*5.94*	*11.61*	*17.69*	*24.71*	-	*-57.10*	-	*-59.76*
	DTSA-II	15.90	28.32	45.79	64.83	-	4.67	-	5.59
	PENEPMA	16.62	29.53	47.68	67.47	-	9.15	-	9.89
	GMRFilm	15.44	26.79	42.13	58.41	-	-0.97	-	-4.87

Table 9 Al film thicknesses calculated using bulk elemental density and for a reduced density of 2.00 gcm-3, and their percentage difference from the FIB section measured thicknesses. Numbers in brackets are interpolated values.

Even after recalculating for a reduce film density the FTM values still show a 60% error relative to FIB. It is proposed that this remaining significant component of the FTM thickness discrepancy is due to the requirement for a large tooling factor (2.0) to compensate for the FTM sensor not being co-located with the samples in the sputter chamber. This issue has certainly been recognised before (Jurek et al. 1994). This factor therefore constitutes a potential major source for error.

Cu on Bi

Previous studies have also found that thin Cu coatings can exhibit reduced densities. For example, Blois and Reiser (1954) found a density of ~7 gcm^{-3} for their thinnest Cu films (~20 nm). However, unlike the Al on Bi samples the calculated Cu thicknesses, in particular those from DTSA-II and GMRFilm, agree very closely with the one FIB data point so there is no evidence to suggest that the 5 – 20 nm Cu coatings in this study have anything lower than the assumed bulk density of 8.96 gcm^{-2}.

Although the FTM values for these samples agree much more closely with the calculated and FIB values than for the Al on Bi samples, there is still a not insignificant 10 – 20% discrepancy at low accelerating voltages (Figure 3b). It appears that, although a co-located FTM sensor is less error prone than a side-located sensor, there is still a sensitivity to differences in sample heights.

Conclusions

Surface films, whether deliberately applied or adventitious surface oxides, provide a significant challenge and potential limitation for low voltage quantitative analysis.

In-coater FTM measurements of film thickness are a major potential source of error, and have knock-on effects for the quantification of the substrate at low accelerating voltages. The 70% over-estimation of the Bi Mα k-ratio when using the FTM value for the '20nm' Al film on Bi at 5 kV renders quantification of the substrate almost meaningless. The errors can be reduced by calculation of the film thickness from measurement of the coating k-ratios,

but at low accelerating voltages the errors in the film thickness and consequently quantification of the substrate can still be as large as 10 – 20%.

For film thickness determination the three software packages used, GMRFilm, DTSA-II and PENEPMA, all provided very similar results, despite the very large differences in time and computing power required. However, for substrate quantification the higher fidelity DTSA-II and PENEPMA tend to provide more accurate results at intermediate voltages. However, at low accelerating voltages, this trend is not clear, with no one method consistently producing better results.

Over the range of film thicknesses and accelerating voltages modelled both the substrate and coating k-ratios show essentially linear trends as functions of the film thicknesses. For simple systems this allows for both parameters to be interpolated from a few pre-calculated data points.

Comparison of the directly measured film thicknesses from FIB sections with the modelled mass thicknesses indicates that the deposited Al films have a much lower than bulk density, in the region of $2gcm^{-2}$. In contrast, the Cu films appear to have the same densities as bulk Cu. Use of mass thickness as opposed to separate thickness and density values would negate any issue of unknown or uncertain densities: both electron energy loss and x-ray absorption calculations are based on mass thickness values and compositions.

Regardless of the coating used the results presented here show that, to minimise the impact on the substrate quantification, the thinnest possible coating that still provides reliable electrical conduction should be used. For C evaporated coatings the very distinctive violet colour of a polished brass witness block when 20 nm of coating is reached makes it a useful and repeatable thickness to use, even though 10 or even 5 nm can provide sufficient conduction on a flat surface. An FTM offers the potential to maintain a reliably thin coating once the operator has determined what that thickness should be.

Acknowledgements

The authors would like to thank AWE for their financial support and Leica UK for the loan of their coaters which were used as part of this study.

References

Anderson, C.A., 1966. Electron Probe Microanalysis of Thin Layers and Small Particles with Emphasis on Light Element Determinations. In T. D. McKinley, K. F. J. Heinrich, & D. B. Wittry, eds. *The Electron Microprobe*. New York: John Wiley and Sons, Inc., pp. 58–74.

Bastin, G.F. et al., 1998. In-Depth Profiling with the Electron Probe Microanalyzer. In X. Llovet & F. Salvat, eds. *Proceedings of EMAS '98 3rd Regional Workshop*. Barcelona: Universitat de BArcelona, pp. 25–55.

Bastin, G.F. & Heijligers, H.J.M., 2000a. A Systematic Database of Thin-Film Measurements by EPMA, Part I – Aluminum Films. *X-Ray Spectrometry*, 29(3), pp.212–238. Available at: http://dx.doi.org/10.1002/(SICI)1097-4539(200005/06)29:3%3C212::AID-XRS422%3E3.0.CO;2-K.

Bastin, G.F. & Heijligers, H.J.M., 2000b. A Systematic Database of Thin-Film Measurements by EPMA, Part II - Palladium Films. *X-Ray Spectrometry*, 29(3), pp.373–397.

Bastin, G.F. & Heijligers, H.J.M., 1991. Quantitative Electron Probe Microanalysis of Nitrogen. *Scanning*, 13, pp.325–342.

Blois, M.S. & Rieser, L.M., 1954. Apparent density of thin evaporated films. *Journal of Applied Physics*, 25(3), pp.338–340.

Bottomley, P.D.W. et al., 2000. EPMA of melted UO2 fuel rods irradiated to a burn-up of 23 GWd/tU. *Mikrochimica Acta*, 132(2–4), pp.391–400.

Campos, C.S. et al., 2001. Metallic thin film thickness determination using electron probe microanalysis. *X-Ray Spectrometry*, 30, pp.253–259.

Goldstein, J. et al., 2003. *Scanning Electron Microscopy and X-Ray Microanalysis* Third., New York: Springer Science + Business Media.

Hartman, T.E., 1965. Density of Thin Evaporated Aluminum Films. *Journal of Vacuum Science and Technology*, 2(5), p.239.

Hutchins, G.A., 1966. Thickness Determination of Thin Films by Electron Probe Microanalysis. In T. D. McKinley, K. F. J. Heinrich, & D. B. Wittry, eds. *The Electron Microprobe*. New York: John Wiley and Sons, Inc., pp. 390–404.

Jurek, K., Renner, O. & Krouský, E., 1994. The role of coating densities in X-ray microanalysis. *Mikrochimica Acta*, 114–115(1), pp.323–326.

Kerrick, D.M., Eminhizer, L.B. & Villaume, J.F., 1973. The Role of Carbon Film Thickness in Electron Microprobe Analysis. *American Mineralogist*, 58, pp.920–925.

Leder, L.B. & Suddeth, J.A., 1960. Characteristic energy losses of electrons in carbon. *Journal of Applied Physics*, 31(8), pp.1422–1426.

Limandri, S.P., Carreras, A.C. & Trincavelli, J.C., 2010. Effects of the Carbon Coating and the Surface Oxide Layer in Electron Probe Microanalysis. *Microscopy and Microanalysis*, 16(5), pp.583–593. Available at: http://journals.cambridge.org/action/displayAbstract?fromPage=online&aid=7907696&fileId=S1431927610093761.

Llovet, X. & Salvat, F., 2016. PENEPMA: a Monte Carlo programme for the simulation of X-ray emission in EPMA. *IOP Conference Series: Materials Science and Engineering*, 109, p.12009. Available at: http://stacks.iop.org/1757-899X/109/i=1/a=012009?key=crossref.a51935eedff3118ec3e813133d747cf3.

Love, G., Cox, M.G.C. & Scott, V.D., 1974. Electron probe microanalysis using oxygen x-rays : II . Absorption correction models. *J. Phys. D: Appl. Phys.*, 7, pp.2142–2155.

Lovell, S. & Rollinson, E., 1968. Density of Thin Films of Vacuum Evaporated Metals. *Nature*, 218(5147), pp.1179–1180. Available at: http://dx.doi.org/10.1038/2181179a0.

Pouchou, J.-L. & Pichoir, F., 1990. Surface Film X-Ray Microanalysis. *Scanning*, 12(4), pp.212–224.

Ritchie, N.W.M., Davis, J. & Newbury, D.E., 2008. DTSA-II: A New Tool for Simulating and Quantifying EDS Spectra - Application to Difficult Overlaps. *Microscopy and Microanalysis*, 14(S2), pp.1176–1177. Available at: http://www.journals.cambridge.org/abstract_S143192760808361X.

Salvat, F., 2015. PENELOPE-2014. A Code System for Monte Carlo Simulation of Electron and Photon Transport. Available at: http://www.oecd-nea.org/lists/penelope.html.

Statham, P.J., 2010. Feasibility of X-ray analysis of multi-layer thin films at a single beam voltage. *IOP Conference Series: Materials Science and Engineering*, 7, p.12027. Available at: http://stacks.iop.org/1757-899X/7/i=1/a=012027?key=crossref.e91d896b62efc586b6d12d593b386394.

Statham, P.J., Llovet, X. & Duncumb, P., 2012. Systematic discrepancies in Monte Carlo predictions of k -ratios emitted from thin films on substrates. *IOP Conference Series: Materials Science and Engineering*, 32, p.12024. Available at:

http://stacks.iop.org/1757-899X/32/i=1/a=012024?key=crossref.3f02c17570d736364c540de44b417b91.

Waldo, R.A., 1988. An Iteration Procedure to Calculate Film Compositions and Thicknesses in Electron-Probe Microanalysis. In D. E. Newbury, ed. *Microbeam Analysis*. San Francisco: San Francisco Press, pp. 310–314.

Walker, C.T., 1999. Electron probe microanalysis of irradiated nuclear fuel : an overview. *Journal of Analytical Atomic Spectrometry*, 14(October 1998), pp.447–454.

Yakowitz, H., 1968. Evaluation of Specimen Preparation and the Use of Standards in Electron Probe Microanalysis. In *50 Years of Progress in Metallographic Techniques*. Philadelphia: American Society for Testing of Materials, pp. 383–408.

Yakowitz, H. & Newbury, D.E., 1976. A Simple Analytical Method for Thin Film Analysis with Massive Pure Element Standards. In *Proceedings of the 9th Annual Scanning Electron Microscope Symposium, Vol. 1*. Chicago: IITRI, pp. 151–152.